Published in final edited form as:

Am J Med Genet A. 2023 January ; 191(1): 90–99. doi:10.1002/ajmg.a.62991.

ALDH1A2-related disorder: A new genetic syndrome due to alteration of the retinoic acid pathway

Eyby Leon[1], **Claris Nde**[2], **Randall S. Ray**[1], **Diego Preciado**[3], **Irene E. Zohn**[2]

[1]Rare Disease Institute, Children's National Hospital, Washington, DC, USA

[2]Center for Genetic Medicine, Children's National Hospital, Washington, DC, USA

[3]Division of Pediatric Otolaryngology, Children's National Hospital, Washington, DC, USA

Abstract

Aldehyde Dehydrogenase 1, Family Member A2 (ALDH1A2) is essential for the synthesis of retinoic acid from vitamin A. Studies in model organisms demonstrate a critical role for ALDH1A2 in embryonic development, yet few pathogenic variants are linked to congenital anomalies in humans. We present three siblings with multiple congenital anomaly syndrome linked to biallelic sequence variants in *ALDH1A2*. The major congenital malformations affecting these children include tetralogy of Fallot, absent thymus, diaphragmatic eventration, and talipes equinovarus. Upper airway anomalies, hypocalcemia, and dysmorphic features are newly reported in this manuscript. In vitro functional validation of variants indicated that substitutions reduced the expression of the enzyme. Our clinical and functional data adds to a recent report of biallelic *ALDH1A2* pathogenic variants in two families with a similar constellation of congenital malformations. These findings provide further evidence for an autosomal recessive *ALDH1A2*-deficient recognizable malformation syndrome involving the diaphragm, cardiac and musculoskeletal systems.

Keywords

ALDH1A2; diaphragm; malformation; syndrome; tetralogy of Fallot

1 | INTRODUCTION

Retinoic acid (RA) is a morphogen that plays a key role in organogenesis of the developing embryo. During embryonic development, a gradient of RA is established in the trunk of the embryo by precise temporal and spatial expression of enzymes involved in synthesis and degradation of RA from dietary vitamin A (Duester, 2008). RA is synthesized in a series of enzymatic reactions where retinol is first reversibly oxidized to retinaldehyde and

Correspondence Eyby Leon, Rare Disease Institute, Children's National Hospital, 7125 13th Place NW, Washington DC 20012, USA. eleon@childrensnational.org.

AUTHOR CONTRIBUTIONS

The following contributions were made: Clinical and Genetic studies Eyby Leon and Randall S. Ray, functional validation and figure preparation Claris Nde, manuscript preparation Eyby Leon and Irene E. Zohn, supervision and funding Eyby Leon and Irene E. Zohn.

CONFLICT OF INTEREST

The authors declare no conflict of interest.

then enzymes of the aldehyde dehydrogenase 1 family (ALDH1) irreversibly oxidize retinal to RA. The primary ALDH1 enzyme during embryogenesis is aldehyde dehydrogenase 1 family member A2 (ALDH1A2), also known as retinaldehyde dehydrogenase 2 (RALDH2) (Kedishvili, 2016). Once synthesized, RA acts as a ligand for the nuclear RA receptors (RARs) that partner with retinoid X receptors (RXRs). RAR/RXR heterodimers bind to RA-responsive elements and recruit transcriptional coactivators upon ligand binding to initiate transcription of genes involved in proliferation, differentiation, and apoptosis (Blomhoff & Blomhoff, 2006).

Studies in animal model systems demonstrate that expression of *Aldh1a2* is required for development of multiple organ systems including the limbs, gonads, lungs, heart, diaphragm, thymus, craniofacial, and feeding apparatus (Clagett-Dame & DeLuca, 2002). Embryos homozygous for null alleles of *Aldh1a2* succumb at early embryonic stages with developmental delays and multiple severe morphological abnormalities of the hindbrain, heart, vasculature, body axis, and limbs (Duester, 2008). Hypomorphic pathogenic variants in *Aldh1a2* or rescue of early developmental defects by supplementation with all-trans-RA do demonstrate a role for *Aldh1a2* in the development of numerous organ systems, implicating this gene in developmental defects such as micrognathia, conotruncal heart anomalies, dysphagia, absent thymus, lung hypoplasia and agenesis, congenital diaphragmatic hernia (CDH), enteric nervous system defects and limb malformations (Niederreither & Dollé, 2008).

In humans, we know that the orally active RA derivative, isotretinoin, used in the treatment of severe cystic acne, is teratogenic (Coberly et al., 1996). A wide spectrum of birth defects including craniofacial, heart, and nervous system malformations have been described with prenatal exposure to this drug (Dai et al., 1992; de la Cruz et al., 1984). A recent review of vitamin A in pregnancy performed by Bastos Maia et al. (2019) describes several human studies indicating how vitamin A deficiency has been linked with fetal growth restriction and congenital anomalies such as CDH. Research in Zebrafish and mouse models reveals that the regulated expression of *Aldh1a2* plays a crucial role in buffering environmental changes in RA exposures, and teratogenesis occurs when this buffering capacity is overrun (D'Aniello et al., 2013; D'Aniello & Waxman, 2015; Lee et al., 2012; Shannon et al., 2017). Exposure to excessive levels of vitamin A during embryogenesis triggers hyperactivation of feedback loops which subsequently over-represses *Aldh1a2* expression, resulting in a “pseudo–vitamin A deficient” state (D'Aniello & Waxman, 2015; Shannon et al., 2017). This model nicely accounts for the similarities in phenotypes caused by RA teratogenesis and deficiency.

Despite the clear requirement for *Aldh1a2* in embryonic development in animal models, a few instances of *ALDH1A2* variants are linked to congenital anomalies in humans including CDH, tetralogy of Fallot (TOF), neural tube and kidney defects (Coste et al., 2015; El Kares et al., 2010; Li et al., 2018; Pavan et al., 2009; Steiner et al., 2013; Urbizu et al., 2013). A multiple congenital anomaly syndrome associated with alterations of this gene was recently reported in three patients from two unrelated families, suggesting that hypomorphic variants may contribute to malformations in humans (Beecroft et al., 2021). Here we present an

additional three siblings with loss of function *ALDH1A2* variants that co-segregate with a very similar phenotypic spectrum.

2 | METHODS

2.1 | Exome and gene sequencing

Trio whole exome sequencing and analysis were done by Baylor Miraca Genetics Laboratories (Houston, TX) on the Illumina HiSeq platform using blood samples from subjects 1 and 2 and both parents. Data analysis and interpretation were done using the Mercury pipeline (https://www.hgsc.bcm.edu/software/mercury). Targeted familial variant gene analysis via massive parallel (NextGen) sequencing with 150 bp paired-end reads on the Illumina NovaSeq 6000 Sequencing System was performed on subject 3 at Children's National Hospital Molecular Laboratory in Washington, DC.

2.2 | Generation of human ALDH1A2 expression constructs

Human *ALDH1A2* expression plasmids used for functional assays were purchased from GenScript. The 1569 bp *ALDH1A2* gene cDNA ORF clone sequence was synthesized from the NCBI Reference Sequence Database (Accession No: NM_003888.4) and cloned into the Kpnl/BamHI site of pcDNA3.1(+)-N-HA vector (Clone ID: OHu19191C). The c.759delC and c.1040G > A genetic variants that model two rare changes in the *ALDH1A2* gene seen in the first 2 subjects were generated based on the reference sequence. Plasmids were transformed into top 10 competent bacteria for plasmid replication and isolated using the QIAGEN Plasmid Kit. The quantity of plasmid DNA was determined by restriction enzyme digestion and Thermo Scientific NanoDrop 2000 Spectrophotometer, respectively.

2.3 | Cell culture and transient transfection assays

HEK293T cells were from American Type Culture Collection (CRL-11268), were maintained in high glucose DMEM media (11995065) supplemented with 10% FBS and Penicillin-Streptomycin, and grown in a 5% CO2 humidified incubator at 37°C. HEK293T cells were transfected using Lipofectamine 3000 Reagent (L3000008) according to manufacturer's instructions.

2.4 | Western blot analysis

Seventy-two hours post-transfection, cells were lysed with Pierce IP Lysis Buffer (87787) supplemented with Halt Protease Inhibitor Cocktail (78429) on a rocker in the cold room for 10 min. Cell debris was removed by centrifugation at 13,000 × g for 10 min at 4°C. The supernatant was transferred into fresh tubes and saved at −80°C until assayed. Total protein was measured using the Pierce BCA Protein assay kit (23225). 15 ug of protein was resolved per lane of a ten-well NuPAGE 4 to12%, Bis-Tris, Mini Protein gel (NP0321) with the NuPAGE MES SDS Running buffer (NP0002) or a 10-well NuPAGE 3 to 8%, Tris-acetate Mini Protein Gel (EA0375) with NuPAGE Tris-Acetate SDS Running Buffer (LA0041). Proteins were transferred to Low-Fluorescence PVDF Transfer Membrane (22860), and western blotting was performed using the Intercept (TBS) system: Blocking Buffer (927–60,001) and Antibody Diluent (927–65,001) and IRDye 800CW donkey anti-mouse (92,632,212; 1:15000 dilution). The primary antibodies used were anti-HA.11

Epitope Tag monoclonal antibody (1:1000 dilution, Clone 16B12, BioLegend) and GAPDH (14C10) Rabbit mAb (#2118, Cell Signaling). Chameleon Duo Prestained protein ladder (928–60,000, LI-COR).

Western blots were visualized using the LiCor Odyssey CLX imaging system and LI-COR software. Relative protein expression was quantitated in five independent experiments using Image Lab Software according to manufacturer instructions. All data sets were analyzed for statistical differences and significance using an unpaired *t*-test (Prism 9). All values are reported as mean with standard deviation.

2.5 | Immunofluorescence assay

Forty-eight hours post-transfection, HEK293T cells were washed with PBS and fixed in 4% PFA for 20 min. Coverslips were blocked with blocking buffer (1% HI Goat Serum, 0.1% Triton-X 100 in 1X PBS) for 1 h and subjected to immunofluorescence analysis using the anti-HA.11 Epitope Tag monoclonal antibody (1:1000 dilution, Clone 16B12, BioLegend), goat anti-mouse Alexa 555 (1:250 dilution, A32727, Thermo Fisher), and Hoechst (1:500 dilution, Sigma) and mounted on glass slides with Fluoromount-G mounting medium (00495802, Thermo Fisher). Images were acquired using the 40X objective on an Olympus BX63 Fluorescence Microscope and analyzed using the Fiji imaging processing package.

Semi-quantification for Immunofluorescence intensity was measured for transfected cells as follows: first, the cell of interest was selected using the drawing/selection tools; then, “set measurement” was selected from the “analyze” menu. In the “set measurement” popup box, area integrated intensity and mean gray value was selected. The fluorescence for each cell was quantified using the “Measure” command under the “Analyze” table A region without fluorescence next to the cell of interest was selected for background measurement using the drawing tool and size was taken as described above. This was repeated for five cells per frame for a total of 25 cells. Finally, background fluorescence was corrected using the formula, corrected total cell fluorescence (CTCF) = integrated density – (area of selected cell X mean fluorescence of background readings). Graphs were generated using Prism 8. Corrected total cell fluorescence (CTCF) was measured only for transfected cells. All values are reported as mean with standard deviation and significance determined using the unpaired *t*-test (Prism 8) with a threshold of $p < 0.05$.

3 | CASE REPORTS AND LABORATORY RESULTS

3.1 | Subject 1

The proband is a male with prenatal history of bilateral talipes equinovarus (TEV) detected on ultrasound at 19 weeks of gestation. The fetal echocardiogram was normal as well as karyotype analysis from amniocentesis was performed at 21 weeks. The patient was born at 40 weeks by vaginal delivery from a gravida 2 para 1, a 21-year-old mother, and 23-year-old father from Honduras and El Salvador, respectively. Birth weight was 3.21 kg (30th centile), head circumference 35 cm (35th centile), length 47 cm (12th centile) and Apgar scores were 7 and 9. After delivery, he developed respiratory distress, oliguria, and hypotension. The

patient was intubated and was placed on inhaled nitric oxide, dopamine drip, and stress dose hydrocortisone. Blood and platelet transfusions were given for anemia (12.4 g/dL) and thrombocytopenia (42 k/ul).

The initial physical exam was remarkable for hypotonia, micrognathia, webbed neck, narrow thorax, bilateral inguinal hernias, undescended testicles, bilateral TEV, and toe syndactyly. Chest X-ray (CXR) showed an abnormal position of the diaphragm due to bilateral congenital diaphragmatic eventrations, confirmed with an ultrasound of the chest and abdomen. Echocardiogram showed a large patent ductus arteriosus (PDA) with patent foramen ovale (PFO). He failed extubation twice, after PDA ligation at 3 weeks of life, and bilateral diaphragmatic plication was done at 1-month-old. Due to persistent need for ventilatory support, laryngoscopy was performed at 1.5 months which showed laryngomalacia with shortened aryepiglottic folds, hooding of arytenoids, and left true vocal fold paralysis prompting a tracheostomy tube placement at 2.5 months. He also had a Nissen fundoplication with gastrostomy tube placement due to persistent emesis on nasogastric (NG) feeds after plication along with bilateral inguinal hernia repair. Electromyography and a brain/spine MRI were normal. He was discharged from the NICU at 3 months of age.

The patient had several admissions for respiratory distress due to pneumonia or tracheitis starting at 5 months of age. He was given an aggressive therapy of systemic and inhaled steroids and bronchodilators and placed on continuous positive airway pressure (CPAP) therapy at 9 months. He began caping his tracheostomy at age 2, but because of continued admissions for respiratory infections, he required mechanical ventilation at night which was discontinued at age 5. He then underwent a sleep study with the trach capped which revealed severe obstructive sleep apnea that prompted an adenotonsillectomy. Direct laryngoscopy and bronchoscopy (DLB) demonstrated a grade 4 view of the larynx due to arytenoid prolapse, retroflexed epiglottis, and proximal tracheomalacia to the tracheostomy stoma. A left arytenoidectomy with supraglottoplasty was performed at age 7 along with downsizing of the tracheostomy tube. A laryngeal tracheal reconstruction due to tracheal collapse at the site of the stoma was performed before successful decannulation.

A bilateral percutaneous heel cord lengthening was performed at 8 months of age, then at ages 2 and 4. He also had bilateral foot posterior capsulotomy as well as posterior tibialis recession with tendon transfer at age 4. His first genetics outpatient evaluation was at 20 months of age where his weight was 11.24 kg (25th centile), height was 85.5 cm (72nd centile), and head circumference was 46.5 cm (12th centile). Additional physical features included epicanthal folds, diastema, everted lips, slopping shoulders, winged scapula, and decreased muscle bulk on lower legs (Figure 1). He had a normal creatine kinase (CK) level. The patient walked at 14 months and his first words were at age 3. At age 7 years, he can speak in 2–3 word phrases and understands English and Spanish. He finished 1st grade in regular classes and receives physical and speech therapies. However, he has not returned to school due to his multiple procedures and risk for infection during the COVID-19 pandemic. He has not had a formal developmental evaluation yet. The patient will have a bilateral orchiopexy soon, his right testis is retractile and his left testis is palpable in the left inguinal canal.

3.2 | Subject 2

Subject 2 is a female younger sibling who was born at 40 weeks via uncomplicated spontaneous vaginal delivery to a 25-year-old gravida 3 para 2 mother and 27-year-old father. The mother reports taking prenatal vitamins as well as levetiracetam and lamotrigine for epilepsy throughout the pregnancy. Early fetal ultrasound showed bilateral TEV. Fetal echocardiograms at 27 and 34 weeks of gestation showed TOF. Non-invasive prenatal testing was negative. Birth weight was 3.2 kg (33rd centile), head circumference was 33.5 cm (19th centile), and length was 49.5 cm (50th centile). Apgar scores were 3 and 9 at 1 and 5 min of life, respectively. After delivery, the patient developed tachycardia, and hypoxemic respiratory distress with PO feeds, so she was placed on CPAP 21% and a nasogastric tube was placed.

The initial physical exam was remarkable for hypotonia, cardiac murmur, micrognathia, and bilateral TEV. After 4 days on CPAP, she developed worsening desaturation episodes and tachycardia to the 270 s, so she was transitioned to a high-flow nasal cannula. Electrophysiological analysis revealed reentrant supraventricular tachycardias and she was started on digoxin for rate control. Early CXR showed shunting vasculature with mild cardiomegaly, but an otherwise grossly normal cardiac silhouette and diaphragm. Echocardiogram and cardiac MRI confirmed TOF with minimal pulmonary stenosis, large ventricular septal defect (VSD) with minimal anterior malalignment, large PDA, a small atrial septal defect (ASD), absent thymus and persistent left superior vena cava. She had a negative SNP chromosomal microarray.

At the time of her intubation for cardiac MRI, the patient was found to have a critical airway with a grade 2–3 view and required multiple intubation attempts by the otolaryngology service. She developed stridor following extubation and was reintubated until PDA ligation was done at 2 weeks of age. VSD repair with non-transannular patch and fenestrated ASD closure was completed at 4 weeks of life. After these procedures, she was still unable to be extubated despite multiple attempts due to laryngomalacia, transglottic edema, subglottic stenosis, and vocal cord paresis seen on DLB. Speech therapy also found poor suck and swallow coordination and assessed her as being at high risk for aspiration, so tracheostomy and gastrostomy tubes were placed simultaneously at 8 weeks of age.

The patient was discharged to a rehabilitation center at 10 weeks old. She transitioned home on 24-h ventilatory support at around 4 months old. Starting at 6 months of age, she had multiple emergency room visits and hospitalizations for emesis and respiratory distress in the setting of viral infections. She had one hospitalization for concurrent methicillin-susceptible staphylococcus aureus pneumonia and pseudomonas tracheitis at 7 months of age. Respiratory illnesses were treated with increased ventilatory support, antibiotic therapy, inhaled corticosteroids, and bronchodilators. Emesis was treated with ondansetron and proton pump inhibitors. She was taking furosemide for congestive heart failure related to TOF. She had bilateral long-leg clubfoot casts placed at 7 months, and lightweight boots and bar at 8 months. At her last genetics outpatient evaluation at 8 months, all of her growth parameters were below the 1st centile, weight of 5.35 kg, length of 63.7 cm, and head circumference of 40.5 cm. Additional physical findings included epicanthal folds, slopping

shoulders, winged scapula, underdeveloped calves, brachydactyly of the fingers, and toe syndactyly (Figure 2).

At 19 months old, she presented to the emergency department in cardiorespiratory arrest, dusky in appearance and with fixed and dilated pupils after being found down at home. Resuscitation efforts failed and she was pronounced dead in the emergency department. An autopsy revealed evidence of acute on chronic aspiration pneumonia, bilateral pulmonary edema and congestion, focally constrictive bronchiolitis, and right heart dilation with overriding aorta and pulmonary stenosis. These findings were consistent with progression of her known congestive heart failure and pulmonary conditions arising from her dysmorphic airway, aspiration, chronic respiratory failure, and ventilatory-associated infections. Mother indicated that she was not able to walk or talk due to significant weakness. Formal developmental evaluation was not performed.

3.3 | Subject 3

1-month-old girl born full term by vaginal delivery with APGARs 8 and 8. The couple had another healthy boy born between Subjects 2 and 3. Prenatal history was remarkable for diagnosis of TEV and TOF, which were confirmed postnatally. Birth weight was 2.9 kg (23rd centile), head circumference was 33.0 cm (23th centile), and length was 48.5 cm (36th centile). She was intubated on her first day of life due to stridor, however, DLB showed normal airway anatomy. She tolerated low ventilator settings and pressure support trials, however, she failed three extubation attempts and was reintubated with a 3.0 ETT. She had a critical airway due to airway inflammation and edema. She was not tolerating NG feeds due to emesis, so she was started on nasoduodenal feeds. At 3 weeks of age, she was found to have hypocalcemia with normal PTH and vitamin D levels, which is controlled with calcium supplementation. She was transferred to the cardiac intensive care unit (CICU) and had a placement of a PDA stent at 1 month.

Physical exam was limited due to tube placement and lines, but flexed halluces were noticed. She had a tracheostomy and GT placement with Nissen fundoplication at 40 days of life. MRI of the brain and neck showed a subacute lacunar infarction involving the subcortical white matter of the left frontal lobe, mild thinning of the corpus callosum, cerebral white matter, and pontine volume loss versus hypoplasia along with mild congenital segmentation anomaly at C2–C3 with hypoplastic intervertebral disc and possible mild vertebral hypoplasia; normal abdominal ultrasound. She had a cardiac arrest due to tracheostomy displacement at 3-months-old during her stay in the CICU awaiting optimal weight gain for cardiac surgery. She had her TOF repaired with a transannular patch, VSD closure, and PFO enlargement without complications at 4-months-old. She is currently off vasoactives, tolerating full feeds, and is expected to be discharged home at almost 5 months of age.

3.4 | Laboratory results

Trio whole-exome sequencing detected biallelic variants of unknown clinical significance in *ALDH1A2* that co-segregated with congenital defects in the first two affected siblings. The chr15: 58284941; NM_003888.3: c.759delC; p.(H253Qfs * 4) variant results in a

frameshift and predicted truncation of the 518 amino acid protein after amino acid 257 and was inherited from the mother. The chr15: 58256129; NM_003888.3: c.1040G > A; p.(Arg347His) variant was inherited from the father and was previously identified in another family (Beecroft et al., 2021). Targeted familial variant gene analysis was performed on subject 3 which identified the two *ALDH1A2* variants; see pedigree in Figure 3a. Her chromosome microarray was negative.

To test if the expression of ALDH1A2 is altered by p.(Arg347His) and p.(H253Qfs * 4) changes, HA-tagged ALDH1A2 constructs with the sequence variants were transfected into HEK293T cells, and expression levels of the proteins were measured by western blot analysis. No detectable expression of the frameshift variant was found, suggesting the protein fragment is not stable (Figure 3b). In contrast, the p.(Arg347His) variant was detectable, but expression levels were significantly reduced when compared to wild type ($p < 0.0001$) (Figure 3b, c). To determine if the p.(Arg347His) sequence variant alters protein localization, the expression of tagged proteins was visualized in HEK293T cells in an immunofluorescence assay. While the sequence variant did not change the intracellular localization of ALDH1A2, a significant decrease (2.3-fold) in the expression of ALDH1A2 was observed (Figure 3d, e).

4 | DISCUSSION

Our findings of co-segregation of loss of function variants in *ALDH1A2* in a multiple congenital anomaly syndrome affecting these three siblings add to another recent report (Beecroft et al., 2021), establishing an *ALDH1A2* deficient malformation syndrome. Altogether, only six affected children and one fetus from three unrelated families have been identified with this newly recognizable syndrome (Table 1).

Common major features are congenital heart disease, musculoskeletal, airway, and diaphragmatic malformations. Our patients expand the phenotype to include malformations of the upper airway, musculoskeletal anatomy, and other dysmorphic features. Airway features include narrowed and malacic upper airway with difficult intubation and the potential for concomitant idiopathic or iatrogenic vocal cord paresis. TEV was the first prenatal finding discovered in all three siblings that were born full term and has been only reported once by Beecroft et al. in the only patient born at term. The winged scapula found in our patients may represent a musculoskeletal or neuromuscular defect that has not been previously described. Significant hypotonia and global developmental delays were significant in subjects 1 and 2. Normal brain MRIs were found in our proband and two previous cases reported by Beecroft et al. However, they also reported one patient showing midline brain defects along with cleft lip and palate thought to be unrelated but subject 3 has mild thinning of the corpus callosum and mild cerebral white matter and pontine hypoplasia. Minor vertebral anomalies, as well as absent, thymus have been found in two patients now as well as undescended testicles (Table 1). Shared dysmorphic features include epicanthal folds, micrognathia, brachydactyly, and toe syndactyly. Our patients did not have lung hypoplasia, which, along with the tracheostomy and gastrostomy tube placements, likely enabled them to survive the neonatal period.

Differential diagnosis includes genetic conditions such as 22q11.2 deletion syndrome that can affect the diaphragm, heart, and thymus. The *TBX1* gene is considered a key gene deleted in 22q11.2 and causes conotruncal heart defects when mutated in humans (Unolt et al., 2017). Numerous studies have uncovered a complex *TBX1* gene regulatory network associated with vitamin A signaling, heart, and diaphragm development. For instance, TBX1 interacts with the transcription factor GATA4 through a conserved GATA-TBX1 regulatory axis (Song et al., 2022). *GATA4* is expressed in the heart and gonads and pathogenic variants in *GATA4* are associated with cardiac and testicular anomalies in humans (Lourenço et al., 2011). Studies in Zebrafish embryos show that overexpression of *gata4* inhibits *aldh1a2* expression (Liang et al., 2012), providing a link to retinoic acid signaling. GATA4 also interacts with ZFPM2 (i.e., FOG2), a multi-zinc-finger transcription factor expressed during heart, brain, and gonad development. This interaction modulates the transcriptional activity of *GATA4* (Bashamboo et al., 2014; De Luca et al., 2011). Heterozygous variants in *ZFPM2* are associated with conotruncal heart defects, specifically tetralogy of Fallot, double outlet right ventricle, and transposition of the great arteries, as well as a congenital diaphragmatic hernia (Ackerman et al., 2005; De Luca et al., 2011). Heterozygous variants in the *ZFPM2* gene have also been reported in individuals with 46,XY disorders of sex development (Bashamboo et al., 2014) like with *GATA4* (Martinez de LaPiscina et al., 2018). *NR2F2* is another gene in the RA pathway to consider since it has been associated to cause CDH, cardiac, and genital anomalies (Bashamboo et al., 2018). Donnai-Barrow syndrome caused by pathogenic variants in the *LRP2* gene which encodes a receptor important for retinol uptake should also be considered since it has a similar phenotype with cardiac defects, lung hypoplasia, CDH along with ocular and brain anomalies. Fryns syndrome should also be in the differential since it has CDH and cardiac defects along with eye and urogenital anomalies (Beecroft et al., 2021).

The probability of being loss-of-function intolerant (pLI) score for *ALDH1A2* is 0.36, indicating this gene is likely under strong selection against loss-of-function variants (Lek et al., 2016). The p.(H253Qfs * 4) variant is predicted to confer loss of function, resulting in a frameshift and truncation of the 518 amino acid protein after amino acid 257. Our data demonstrate a complete absence of gene product when this p.(H253Qfs * 4) variant is expressed in HEK293T cells, suggesting a complete loss of function due to nonsense-mediated decay. The c.1040G > A;p.(Arg347His) variant is rare in gnomAD (allele frequency 3.6×10^5) with no homozygotes identified. It was previously found in a female patient with cardiac defects, lung hypoplasia, and CDH who also had the c.1147G > A;p.(Ala383Thr) variant reported by Beecroft et al. The Arg347 residue is evolutionarily conserved from yeast to humans and predicted to be pathogenic by several in silico tools. Previous functional analysis indicated that the p.(Arg347His) variant is likely a hypomorphic allele with reduced enzymatic activity leading to decreased RA production (Beecroft et al., 2021). Protein modeling revealed that R347 interacts in a network of hydrogen bonds with four other amino acids and substitution to histidine disrupts this network and potentially alters the structure of the protein (Beecroft et al., 2021). Our data add to this characterization and demonstrate that the p.(Arg347His) variant shows reduced protein expression in HEK293T cells, consistent with the hypomorphic activity noted in functional assays.

Multiple lines of evidence support the conclusion that *ALDH1A2* sequence variants are responsible for this newly described multiple congenital malformation syndrome in concordance with the American College of Medical Genetics and Genomics (ACMG) guidance for interpretation of sequence variants (Richards et al., 2015). (1) Sequence variants segregate with the syndrome in three families with five affected individuals. (2) Features of the syndrome have significant overlap with malformations described in multiple vertebrate model systems. (3) Computational evidence supports a deleterious effect of sequence variants including (a) conservation of the altered sequences across evolution, (b) multiple in silico algorithms predict deleterious effect on gene function, (c) molecular modeling suggest sequence substitutions that would disrupt protein function. (4) *ALDH1A2* has a low rate of benign missense variation with rare missense variants in control populations and no homozygous individuals. (5) Experimental functional data indicate that sequence variants result in reduced enzymatic activity of *ALDH1A2* as well as reduced expression.

In conclusion, our study provides further evidence that the *ALDH1A2* gene is responsible for a newly recognizable multiple congenital anomaly syndrome. *ALDH1A2* should be considered when evaluating patients with multiple malformations involving the diaphragm, cardiac and musculoskeletal systems.

ACKNOWLEDGMENTS

The authors would like to thank all the parents who have shared all the medical information needed for this manuscript. Authors also acknowledge Elias Oxman for guidance with functional characterization of *ALDH1A2* sequence variants.

FUNDING INFORMATION

This project was supported in part by R01-HD098861 to IEZ and Award Number P50HD105328 and U54HD090257 from the NIH, District of Columbia Intellectual and Developmental Disabilities Research Center Award (DC-IDDRC) program. The contents are solely the responsibility of the authors and do not necessarily represent the official views of the District of Columbia Intellectual and Developmental Disabilities Research Center or the National Institutes of Health.

DATA AVAILABILITY STATEMENT

The data that support the findings of this study are available on request from the corresponding author. The data are not publicly available due to privacy or ethical restrictions.

REFERENCES

Ackerman KG, Herron BJ, Vargas SO, Huang H, Tevosian SG, Kochilas L, Rao C, Pober BR, Babiuk RP, Epstein JA, Greer JJ, & Beier DR (2005). Fog2 is required for normal diaphragm and lung development in mice and humans. PLoS Genetics, 1(1), 58–65. 10.1371/journal.pgen.0010010 [PubMed: 16103912]

Bashamboo A, Brauner R, Bignon-Topalovic J, Lortat-Jacob S, Karageorgou V, Lourenco D, Guffanti A, & McElreavey K (2014). Mutations in the FOG2/ZFPM2 gene are associated with anomalies of human testis determination. Human Molecular Genetics, 23(14), 3657–3665. 10.1093/hmg/ddu074 [PubMed: 24549039]

Bashamboo A, Eozenou C, Jorgensen A, Bignon-Topalovic J, Siffroi JP, Hyon C, Tar A, Nagy P, Sólyom J, Halász Z, Paye-Jaouen A, Lambert S, Rodriguez-Buritica D, Bertalan R, Martinerie L,

Rajpert-De Meyts E, Achermann JC, & McElreavey K (2018). Loss of function of the nuclear receptor NR2F2, encoding COUP-TF2, causes testis development and cardiac defects in 46, XX Children. The American Journal of Human Genetics, 102(3), 487–493. 10.1016/j.ajhg.2018.01.021 [PubMed: 29478779]

Bastos Maia S, Rolland Souza AS, Costa Caminha MF, Lins da Silva S, Callou Cruz RSBL, Carvalho Dos Santos C, & Batista FM (2019). Vitamin a and pregnancy: A narrative review. Nutrients, 11(3), 681. 10.3390/nu11030681 [PubMed: 30909386]

Beecroft SJ, Ayala M, McGillivray G, Nanda V, Agolini E, Novelli A, Digilio MC, Dotta A, Carrozzo R, Clayton J, Gaffney L, McLean CA, Ng J, Laing NG, Matteson P, Millonig J, & Ravenscroft G (2021). Biallelic hypomorphic variants in ALDH1A2 cause a novel lethal human multiple congenital anomaly syndrome encompassing diaphragmatic, pulmonary, and cardiovascular defects. Human Mutation, 42(5), 506–519. 10.1002/humu.24179 [PubMed: 33565183]

Blomhoff R, & Blomhoff HK (2006). Overview of retinoid metabolism and function. Journal of Neurobiology, 66(7), 606–630. 10.1002/neu.20242 [PubMed: 16688755]

Clagett-Dame M, & DeLuca HF (2002). The role of vitamin a in mammalian reproduction and embryonic development. Annual Review of Nutrition, 22, 347–381. 10.1146/annurev.nutr.22.010402.102745E

Coberly S, Lammer E, & Alashari M (1996). Retinoic acid embryopathy: Case report and review of literature. Pediatric Pathology & Laboratory Medicine, 16(5), 823–836. [PubMed: 9025880]

Coste K, Beurskens LW, Blanc P, Gallot D, Delabaere A, Blanchon L, Tibboel D, Labbe A, Rottier RJ, & Sapin V (2015). Metabolic disturbances of the vitamin a pathway in human diaphragmatic hernia. American Journal of Physiology. Lung Cellular and Molecular Physiology, 308(2), L147–L157. 10.1152/ajplung.00108.2014 [PubMed: 25416379]

Dai WS, LaBraico JM, & Stern RS (1992). Epidemiology of isotretinoin exposure during pregnancy. Journal of the American Academy of Dermatology, 26(4), 599–606. 10.1016/0190-9622(92)70088-w [PubMed: 1597546]

D'Aniello E, Rydeen AB, Anderson JL, Mandal A, & Waxman JS (2013). Depletion of retinoic acid receptors initiates a novel positive feedback mechanism that promotes teratogenic increases in retinoic acid [research support, N.I.H., extramural]. PLoS Genetics, 9(8), e1003689. 10.1371/journal.pgen.1003689 [PubMed: 23990796]

D'Aniello E, & Waxman JS (2015). Input overload: Contributions of retinoic acid signaling feedback mechanisms to heart development and teratogenesis [research support, N.I.H., extramural research support, non-U.S. Gov't review]. Developmental Dynamics, 244(3), 513–523. 10.1002/dvdy.24232 [PubMed: 25418431]

De la Cruz E, Sun S, Vangvanichyakorn K, & Desposito F (1984). Multiple congenital malformations associated with maternal isotretinoin therapy. Pediatrics, 74(3), 428–430. [PubMed: 6591112]

De Luca A, Sarkozy A, Ferese R, Consoli F, Lepri F, Dentici ML, Vergara P, De Zorzi A, Versacci P, Digilio MC, Marino B, & Dallapiccola B (2011). New mutations in ZFPM2/FOG2 gene in tetralogy of Fallot and double outlet right ventricle. Clinical Genetics, 80(2), 184–190. 10.1111/j.1399-0004.2010.01523.x. Epub 2010 Aug 2. [PubMed: 20807224]

Duester G (2008). Retinoic acid synthesis and signaling during early organogenesis. Cell, 134(6), 921–931. 10.1016/j.cell.2008.09.002 [PubMed: 18805086]

El Kares R, Manolescu DC, Lakhal-Chaieb L, Montpetit A, Zhang Z, Bhat PV, & Goodyer P (2010). A human ALDH1A2 gene variant is associated with increased newborn kidney size and serum retinoic acid. Kidney International, 78(1), 96–102. 10.1038/ki.2010.101 [PubMed: 20375987]

Kedishvili NY (2016). Retinoic acid synthesis and degradation. Sub-Cellular Biochemistry, 81, 127–161. 10.1007/978-94-024-0945-1_5 [PubMed: 27830503]

Lee LM, Leung CY, Tang WW, Choi HL, Leung YC, McCaffery PJ, Wang CC, Woolf AS, & Shum AS (2012). A paradoxical teratogenic mechanism for retinoic acid [research support, non-U.S. Gov't]. Proceedings of the National Academy of Sciences of the United States of America, 109(34), 13668–13673. 10.1073/pnas.1200872109 [PubMed: 22869719]

Lek M, Karczewski KJ, Minikel EV, Samocha KE, Banks E, Fennell T, O'Donnell-Luria AH, Ware JS, Hill AJ, Cummings BB, Tukiainen T, Birnbaum DP, Kosmicki JA, Duncan LE, Estrada K, Zhao F, Zou J, Pierce-Hoffman E, Berghout J Exome Aggregation, C. (2016). Analysis of protein-coding

genetic variation in 60,706 humans. Nature, 536(7616), 285–291. 10.1038/nature19057 [PubMed: 27535533]

Li H, Zhang J, Chen S, Wang F, Zhang T, & Niswander L (2018). Genetic contribution of retinoid-related genes to neural tube defects. Human Mutation, 39(4), 550–562. 10.1002/humu.23397 [PubMed: 29297599]

Liang D, Jia W, Li J, Li K, & Zhao Q (2012). Retinoic acid signaling plays a restrictive role in zebrafish primitive myelopoiesis. PLoS One, 7(2), e30865. 10.1371/journal.pone.0030865 [PubMed: 22363502]

Lourenço D, Brauner R, Rybczynska M, Nihoul-Fékété C, McElreavey K, & Bashamboo A (2011). Loss-of-function mutation in GATA4 causes anomalies of human testicular development. Proceedings of the National Academy of Sciences of the United States of America, 108(4), 1597–1602. 10.1073/pnas.1010257108 [PubMed: 21220346]

Martinez de LaPiscina I, de Mingo C, Riedl S, Rodriguez A, Pandey AV, Fernández-Cancio M, Camats N, Sinclair A, Castaño L, Audi L, & Flück CE (2018). GATA4 variants in individuals with a 46, XY disorder of sex development (DSD) may or may not be associated with cardiac defects depending on second hits in other DSD genes. Front Endocrinol (Lausanne), 4(9), 142. 10.3389/fendo.2018.00142.

Niederreither K, & Dollé P (2008). Retinoic acid in development: Towards an integrated view. Nature Reviews. Genetics, 9(7), 541–553. 10.1038/nrg2340.

Pavan M, Ruiz VF, Silva FA, Sobreira TJ, Cravo RM, Vasconcelos M, Marques LP, Mesquita SM, Krieger JE, Lopes AA, Oliveira PS, Pereira AC, & Xavier-Neto J (2009). ALDH1A2 (RALDH2) genetic variation in human congenital heart disease. BMC Medical Genetics, 10, 113. 10.1186/1471-2350-10-113 [PubMed: 19886994]

Richards S, Aziz N, Bale S, Bick D, Das S, Gastier-Foster J, Grody WW, Hegde M, Lyon E, Spector E, Voelkerding K, Rehm HL, & Committee ALQA (2015). Standards and guidelines for the interpretation of sequence variants: A joint consensus recommendation of the American College of Medical Genetics and Genomics and the Association for Molecular Pathology. Genetics in Medicine, 17(5), 405–424. 10.1038/gim.2015.30 [PubMed: 25741868]

Shannon SR, Moise AR, & Trainor PA (2017). New insights and changing paradigms in the regulation of vitamin A metabolism in development. Wiley Interdisciplinary Reviews: Developmental Biology, 6(3), 1–28. 10.1002/wdev.264

Song M, Yuan X, Racioppi C, Leslie M, Stutt N, Aleksandrova A, Christiaen L, Wilson MD, & Scott IC (2022). GATA4/5/6 family transcription factors are conserved determinants of cardiac versus pharyngeal mesoderm fate. Science Advances, 8(10), eabg0834. 10.1126/sciadv.abg0834 [PubMed: 35275720]

Steiner MB, Vengoechea J, & Collins RT 2nd. (2013). Duplication of the ALDH1A2 gene in association with pentalogy of Cantrell: A case report. Journal of Medical Case Reports, 7, 287. 10.1186/1752-1947-7-287 [PubMed: 24377748]

Unolt M, DiCairano L, Schlechtweg K, Barry J, Howell L, Kasperski S, Nance M, Adzick NS, Zackai EH, & McDonald-McGinn DM (2017). Congenital diaphragmatic hernia in 22q11.2 deletion syndrome. American Journal of Medical Genetics. Part A, 173(1), 135–142. 10.1002/ajmg.a.37980 [PubMed: 27682988]

Urbizu A, Toma C, Poca MA, Sahuquillo J, Cuenca-Leon E, Cormand B, & Macaya A (2013). Chiari malformation type I: A case-control association study of 58 developmental genes. PLoS One, 8(2), e57241. 10.1371/journal.pone.0057241 [PubMed: 23437350]

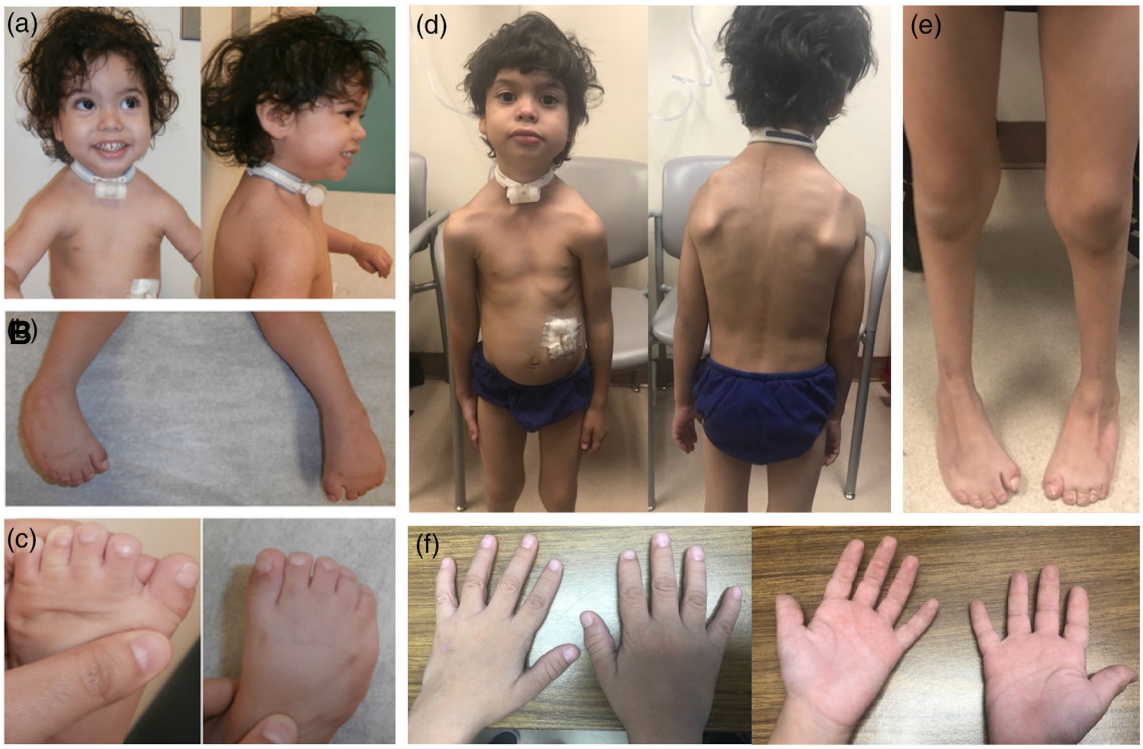

FIGURE 1.
Subject 1. A-C: 20 months of age. D-F: 5 years old

FIGURE 2.
Subject 2. 8 months

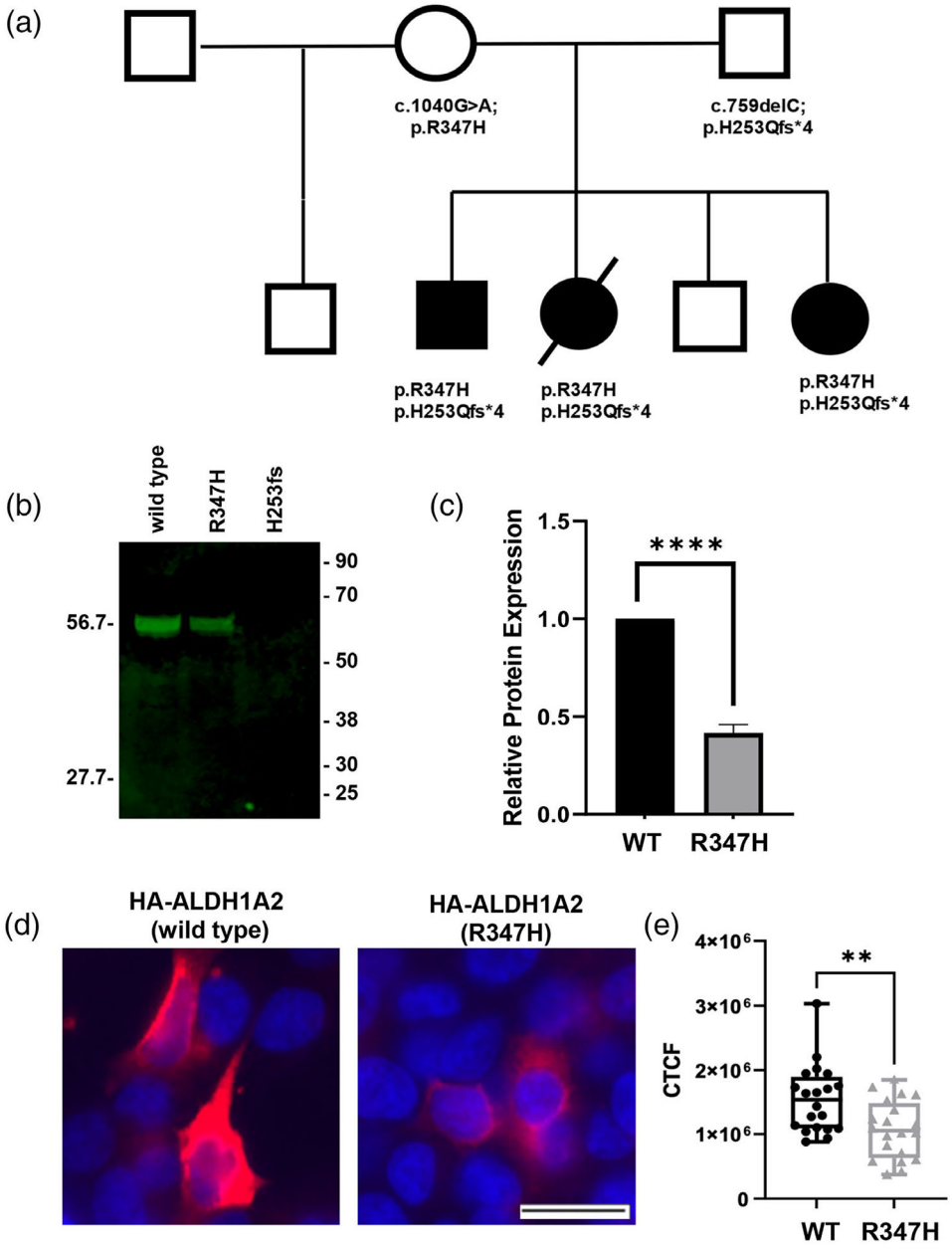

FIGURE 3.

Biallelic ALDH1A2 sequence variants segregate with phenotype and alter expression levels of the gene product. (a). Pedigree showing segregation of developmental syndrome with biallelic *ALDH1A2* sequence variants. (b). The indicated variants were introduced into a mammalian expression construct encoding HA-ALDH1A2 and transfected into HEK293T cells. Western blot analysis reveals reduced expression of the p.(Arg347His) variant and absent expression of p.(H253Qfs * 4). (c). Relative protein expression was quantitated in five independent experiments, ****$p < 0.0001$. (d). Immunofluorescence assay showing reduced expression of the p.(Arg347His) variant. (e). Semi-quantification for

immunofluorescence intensity was measured in 5 cells per frame for a total of 25 cells. Corrected total cell fluorescence (CTCF), $^{**}p < 0.01$

TABLE 1

Clinical features of the affected individuals harboring biallelic ALDH1A2 variants

	Newly reported cases in this manuscript.			***Previously reported by Beercroft* et al.**			
Individual	**Subject 1**	**Subject 2**	**Subject 3**	**AUS1-II:1**	**AUS1-II:3**	**AUS1-II:6**	**ITA1-II:1**
Gestational age	40/40	40/40	40/40	34/40	33 + 3/40	Terminated 13 weeks	Term
Age at death	N/A	19 months	N/A	19 days	1 day	N/A	3 months
Pregnancy	TEV detected at 19 weeks, normal fetal echocardiogram, and normal karyotype from amniocentesis at 21 weeks.	TEV at 20 TOF and 27 weeks gestations. Negative NIPT.	TOF and TEV at 14 weeks	Polyhydramnios, SPROM, abnormal CTG, and born via ECS (34 /40)	↑NT (4.5 mm) 20 weeks polyhydramnios, SPROM, abnormal CTG, Born via ECS (33 + 3 /40)	TNT (9.0 mm), cystic hygroma at 12 weeks	Left congenital diaphragmatic hernia and complex heart defects diagnosed by prenatal ultrasound
Lungs	Normal	Normal	Normal	Hypoplasia	Severe hypoplasia and normal location	ND	Unilateral hypoplasia
Diaphragm	Diaphragmatic eventration.	Normal	Normal	Diaphragmatic eventration	Bilateral diaphragmatic eventration	ND	Diaphragmatic hernia (left)
Thymus	ND	Absent	Absent	ND	Absent	ND	ND
Cardiovascular system	Large PDA with PFO.	TOF, large PDA, a small ASD, and persistent left superior vena cava complicated by reentrant supraventricular tachycardias.	TOF seen on fetal echocardiogram. Born vaginally at full term.	AP window	AP window. interrupted IVC and azygous continuation.	ND	Pulmonary artery hypoplasia, aortic root ectasia, and three aortopulmonary collateral arteries
Brain	Normal brain and spine MRIs.	Increased supratentorial CSF spaces. Mild increase in bitemporal calvarial measurement.	Subacute lacunar infarction involving the subcortical white matter of the left frontal lobe, mild thinning of the corpus callosum, mild cerebral white matter, and pontine volume loss.	Macrocephaly	Macrocephaly	ND	Normal brain MRI
Urogenital features	Undescended testis	ND	ND	Undescende testicles, small kidneys	ND	ND	Normal kidney US
Musculoskeletal features	Bilateral talipes equinovarus, narrow thorax, and syndactyly (toes), bilateral inguinal hernias, slopping shoulders, winged scapula, and decreased muscle bulk on lower legs. Normal electromyography testing	Bilateral talipes equinovarus, slopping shoulders, winged scapulae, underdeveloped calves, brachydactyly of the fingers, and toe syndactyly	Flexed halluces, (physical exam largely inhibited by medical apparatus in intensive care setting). MRI of the neck showed mild congenital segmentation anomaly at C2–C3 with hypoplastic intervertebral disc and mild vertebral hypoplasia.	Syndactyly (fingers and toes)	Syndactyly (fingers and toes) 11 pairs of ribs, coronal clefts of vertebrae.	ND	Bilateral talipes equinovarus

	Newly reported cases in this manuscript.			*Previously reported by Beercroft* et al.			
Individual	**Subject 1**	**Subject 2**	**Subject 3**	**AUS1-II:1**	**AUS1-II:3**	**AUS1-II:6**	**ITA1-II:1**
	and normal creatine kinase levels.						
Facial features	Micrognathia, webbed neck, epicanthal folds, diastema, and everted lips.	Micrognathia, and epicanthal folds.	ND	Low-set ears, micrognathia, and wide-spaced nipples.	Downslanting PFs, and micrognathia (mild).	ND	Bulbous nose, micrognathia, and pterygia.
Additional features	Shortened aryepiglottic folds, hooding of arytenoids, left true vocal cord paralysis	Laryngomalacia, subglottic stenosis.	Hypocalcemia with normal parathyroid hormone and vitamin D levels.	Optic nerve hypoplasia.	Hepatomegaly	ND	ND

Abbreviations: AP, aortopulmonary; CTG, cardiotocograph; ECS, emergency Caesarian section; IVC, inferior vena cava; n/40, weeks gestation; NA, no applicable; ND, not described; NT, nuchal translucency; PDA, patent ductus arteriosus; PF, palpebral fissure; PFO, patent foramen ovale; SPROM, spontaneous premature rupture of membranes; TEV, talipes equinovarus; TOP, termination of pregnancy.